safety

MDPI

Article

A Human-Stiffness-Based Simulator for Ergonomic Evaluation of Pistol-Grip Power Tool Reaction

Raj Arjun, Pranav Bhat and Naveen Chandrashekar *

Department of Mechanical and Mechatronics Engineering, University of Waterloo, Waterloo, ON N2L 3G1, Canada; rajarjun3523@gmail.com (R.A.); pbhat@uwaterloo.ca (P.B.)
* Correspondence: nchandra@uwaterloo.ca

Abstract

Powered pistol-grip fastening tools can produce substantial handle rotation during torque build-up, which may contribute to operator overuse injuries. This study developed and evaluated a human-stiffness-based physical simulator for a controlled relative comparison of fastening variables affecting peak handle rotation. The simulator used a DC-powered pistol-grip tool, which was constrained to rotate about its spindle axis, with a double-acting pneumatic cylinder providing resistance set according to a specified human-derived stiffness. The evaluation used stiffness data from 10 operators at 5 and 7.5 N·m, with simulator peak displacement compared to in vivo measurements using paired analyses. The simulator was then used as a screening platform to examine the effect of target torque and, at 7.5 N·m, the effects of fastener material, drive style, head type, and spindle speed. The simulator overpredicted human peak displacement, with mean biases of 14.72° at 5 N·m and 10.29° at 7.5 N·m. The peak rotation increased by 15.0% when torque was increased from 5 to 7.5 N·m ($p = 0.022$). Torx Plus style fasteners produced 11.5% less rotation than Hex drive fasteners; fastener material significantly affected rotation; head type did not; and rotation was substantially lower at 160 rpm. Although the simulator did not reproduce absolute human displacement without bias, the results support its use as a screening platform for relative comparison under fixed mechanical boundary conditions rather than as an absolute predictor of human displacement or injury risk.

Keywords: pistol-grip power tool; reaction torque; hand–arm biomechanics; upper-extremity stiffness; physical simulator; powered fastening

1. Introduction

Hand-held powered torque tools are widely used to install threaded fasteners in manufacturing assembly operations. DC-powered tools are increasingly used because electric motors, position encoders, and electronic controllers allow spindle motion and applied torque to be controlled with good repeatability [1]. Pistol-grip configurations are particularly common when the location and orientation of the joint make this geometry convenient for the operator. Despite these advantages, powered fastening can expose operators to rapid reaction forces and moments during each tightening cycle. In high-volume manufacturing, where workers may perform hundreds of fastening operations during a shift, repeated exposure to these transient mechanical loads represents an important ergonomic consideration.

A fastening cycle can be considered in three main stages. During rundown, the spindle advances the fastener until it is seated and torque begins to rise. This is followed by

Check for updates

Academic Editor: Raphael Grzebieta

Received: 3 September 2026
Revised: 15 October 2026
Accepted: 26 October 2026
Published: 28 October 2026

Copyright: © 2026 by the authors. Licensee MDPI, Basel, Switzerland. This article is an open access article distributed under the terms and conditions of the Creative Commons Attribution (CC BY) license.

the tightening (or torque build-up) stage, during which the fastener is driven to the programmed target torque. Once the target torque is reached, the controller shuts off the motor and the fastening cycle stops. As torque develops in the fastener, an opposing reaction moment acts on the tool body. For a pistol-grip tool, this reaction tends to rotate the handle about the spindle axis, requiring the operator to resist the motion through the hand, wrist, forearm, and more proximal joints. Because the reaction develops rapidly, the operator may not completely arrest the handle motion before the tool reaches its shut-off torque. This rapid movement is commonly experienced as tool kickback. Previous experimental studies have shown that torque-tool reactions can produce substantial hand–arm forces, muscle activation, displacement, and discomfort [2,3], and higher power tool kinetic exposure in automotive assembly has been associated with increased upper-limb injury risk [4].

From an occupational ergonomics perspective, an important consideration is that the magnitude of the reaction experienced by the operator is not determined by target torque alone. Tool characteristics, torque build-up behavior, joint hardness, working posture, and the mechanical response of the operator can all influence handle displacement [5,6]. Modern DC fastening systems also permit parameters such as the spindle speed, torque-control strategy, and tightening profile to be modified. The characteristics of the fastener and joint can similarly affect how torque develops during tightening. Consequently, two fastening operations reaching the same final torque may produce different transient reactions at the tool handle. Identifying engineering parameters that reduce these reactions could therefore provide opportunities to improve the ergonomic design of industrial fastening operations without necessarily changing the required final tightening torque.

Evaluating these factors directly with human participants presents several challenges. Human responses vary with posture, grip strategy, strength, anticipation, fatigue, and other operator characteristics, making it difficult to isolate the influence of an individual tool or fastening parameter. Systematically evaluating numerous combinations of fasteners, tool settings, and joint characteristics also requires repeated exposure of participants to tool reactions. A physical surrogate that reproduces the relevant mechanical characteristics of the operator can complement human testing by providing a repeatable boundary condition while engineering variables are systematically changed. Such a platform could be particularly useful for screening fastening system designs and identifying conditions that warrant subsequent evaluation with human operators.

Mechanical representations of the human hand–arm system provide a basis for developing such a simulator. Lin and colleagues represented the hand–arm response to power tool reactions using a single-degree-of-freedom system characterized by stiffness, damping, and effective inertia [7–9]. These studies demonstrated that operator mechanical properties vary with the task and working conditions and that these properties can be used to estimate tool motion. Physical simulators have also been developed for right-angle torque tools. Ay et al. characterized human hand–arm dynamics during right-angle tool operation [10] and subsequently developed a dynamic simulator incorporating selected operator mechanical properties for the controlled evaluation of powered torque-tool reactions [11]. However, the kinematics of pistol-grip fastening differ from those of right-angle tools. For a pistol-grip tool, rotation of the handle about the spindle axis is a dominant component of the reaction, requiring a simulator specifically designed to reproduce this motion.

In our previous in vivo study, experienced automotive assembly workers performed DC-powered pistol-grip fastening tasks at different target torques and tool locations, and effective upper-extremity stiffness and damping were estimated from the measured responses [12]. These experimentally derived mechanical properties provide an opportunity to develop a physical surrogate in which the resistance applied to the tool is based on measurements from actual operators rather than an arbitrarily selected mechanical stiffness

value. Once established, such a simulator could provide a controlled platform for investigating how tool and fastening parameters influence handle reaction while eliminating inter- and intra-operator variability during comparative testing.

Therefore, the objectives of the present study were as follows: (1) to develop a physical simulator that reproduces the dominant rotational response of a pistol-grip power tool while applying human-derived mechanical resistance; (2) to evaluate the simulator by comparing peak handle rotation with corresponding in vivo measurements at target torques of 5 and 7.5 N·m; and (3) to demonstrate its application as a controlled ergonomic screening platform by examining the effects of the target torque, fastener material, drive style, head type, and spindle speed on peak tool-handle rotation. The broader aim was to establish a repeatable experimental approach for evaluating engineering factors that influence power tool reactions and that may ultimately inform the ergonomic design of industrial fastening operations.

The intended domain of the current prototype is the bench-top relative screening of pistol-grip fastening configurations under fixed mechanical boundary conditions within the tested torque range. It is not intended to predict an individual worker's absolute handle displacement or musculoskeletal injury risk.

2. Materials and Methods

2.1. Simulator Design and Overall Mechanism

The simulator was designed around several practical requirements derived from the fastening task. It had to allow the pistol-grip tool to rotate about its spindle axis while applying a controllable resistance representative of the operator's upper-extremity stiffness. The design also had to accommodate the axial advance of the fastener during rundown without restricting the rotational motion of the tool. This was achieved using a quick-return mechanism coupled to a translating slider and a spring-loaded joint plate. A double-acting pneumatic cylinder mounted along the guide rail provided the adjustable mechanical resistance, with cylinder pressure set according to the stiffness measured during the in vivo experiments. The tool was held in a custom fixture aligned with the spindle axis, and the joint plate accepted interchangeable fasteners. The arrangement also allowed the production tool, its controller, and its built-in torque and angular displacement measurements to be used directly during simulator testing.

The aluminum guide rail was connected to the main frame by a pivot joint at one end and simply supported in its nominal horizontal position at the other. A cable-and-pulley counterweight was added to compensate for the weight of the tool, holder, and slider; approximately 10 N provided the desired equilibrium. The double-acting pneumatic cylinder was mounted along the guide rail, with its rod connected directly to the slider. This arrangement caused handle rotation to displace the cylinder and generated the opposing force used to represent the operator.

The resulting simulator is shown in Figure 1, and the kinematic mechanism used to relate tool rotation to slider motion is described below.

2.2. Kinematics of the Quick-Return Mechanism

A quick-return mechanism was selected because it simultaneously satisfied two requirements: it constrained tool response to the desired rotation about the spindle axis and provided a linear degree of freedom to which an actuator could be attached. The mechanism contained three revolute joints and one prismatic joint and therefore produced a single prescribed degree of freedom. The spindle-axis joint defined the tool rotation, θ. The pistol-grip handle was connected through a slider to a pivoting guide rail, and the pneumatic cylinder opposed translation of the slider along the rail. Figure 2a shows the kinematic arrangement, and Figure 2b shows its physical implementation in the simulator.

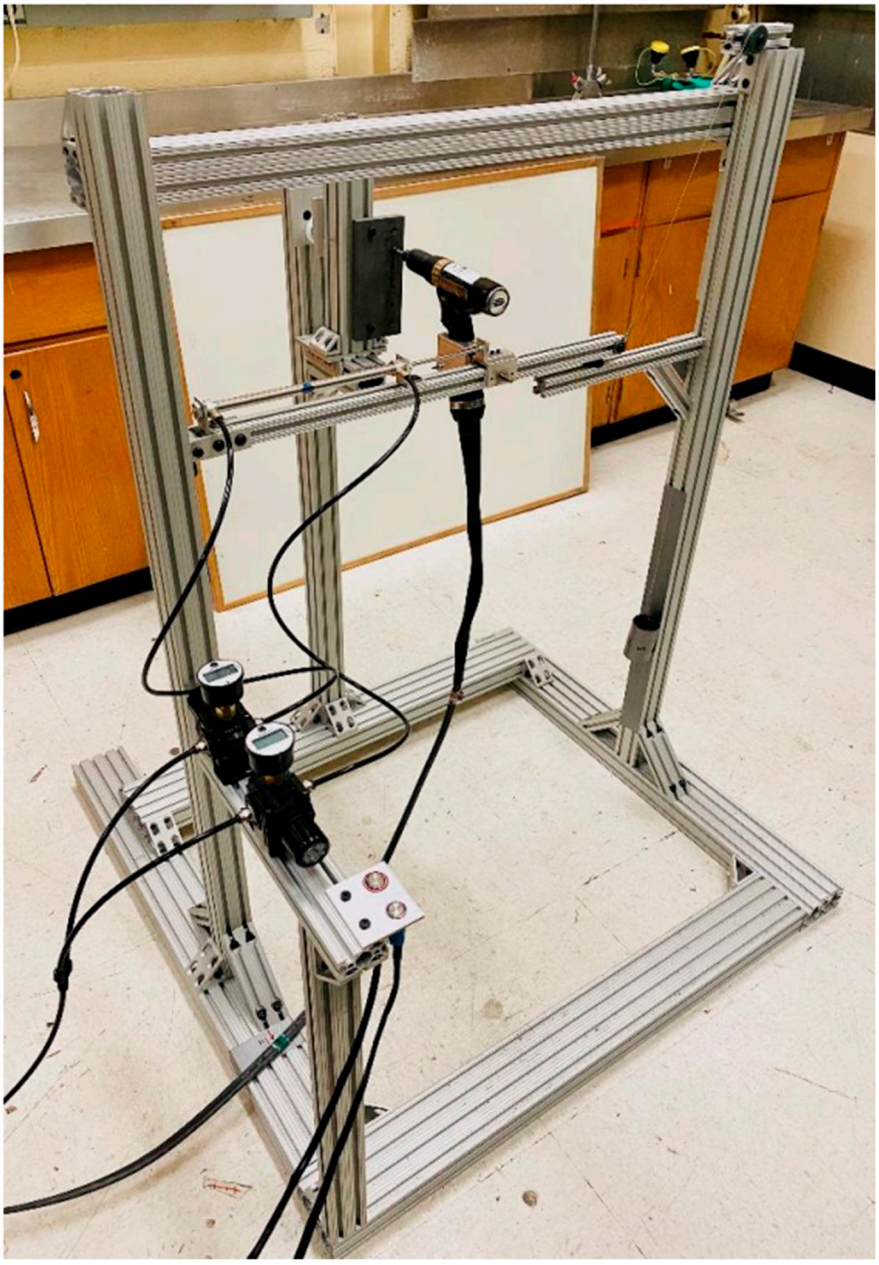


Figure 1. Pistol-grip power tool hand simulator. The double-acting pneumatic cylinder provides the adjustable resistance used to represent operator stiffness.

The geometry was defined using effective handle length h, initial slider distance s_0, instantaneous slider position s, guide rail rotation β, and the fixed distance p between the spindle axis and guide rail pivot. With the tool initially perpendicular to the guide rail, the geometric relation was:

$$p^2 = h^2 + {s_0}^2 = h^2 + s^2 - 2sh\sin(\theta - \beta) \quad (1)$$

which gives:

$$\sin(\theta - \beta) = (s^2 - {s_0}^2)/(2sh) \quad (2)$$

Differentiation of the mechanism geometry related slider velocity to the angular velocity of the tool. Thus, resistance generated linearly by the pneumatic actuator was transmitted through the mechanism as resistance to the rotational displacement of the pistol-grip handle. This mapping allowed the linear stiffness measured at the human hand–tool interface to be

implemented mechanically while preserving the principal rotational response observed during fastening.

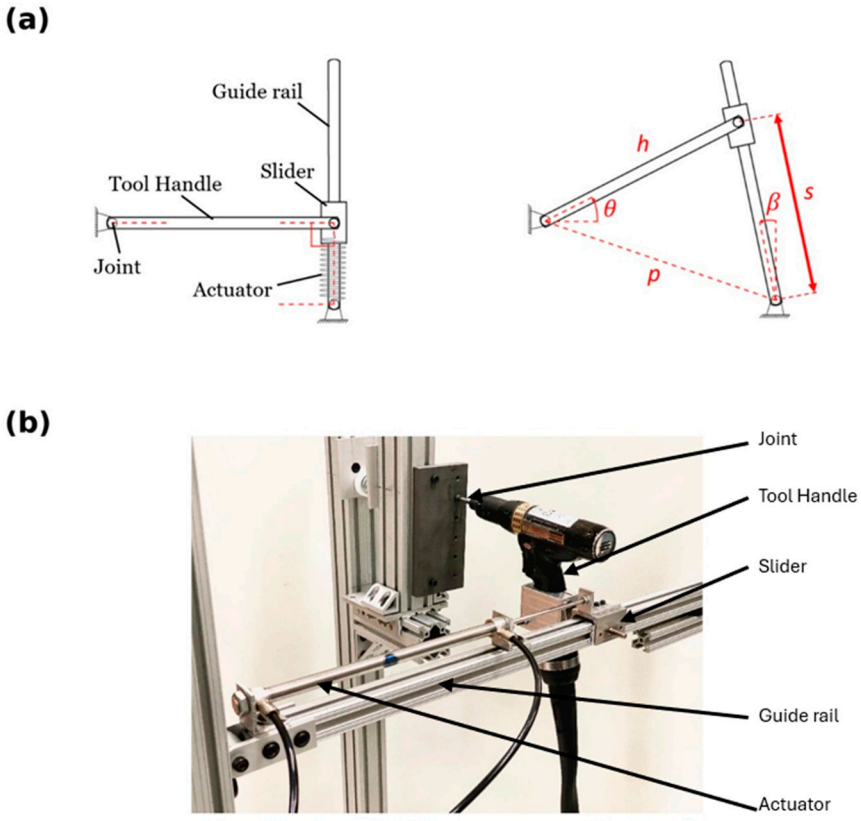


Figure 2. Kinematic design and physical implementation of the simulator. (**a**) Kinematic arrangement, showing the quick-return mechanism relating tool-handle rotation to slider motion. (**b**) Physical implementation with the pistol-grip tool, tool holder, slider, and guide rail identified.

A custom aluminum holder was machined to conform to the pistol-grip contour and distribute clamping load around the handle. The holder was connected to a stainless-steel slider that translated along a 25.4 mm square T-slot guide rail. UHMW polyethylene bearing pads were incorporated to reduce friction. A flanged dry-running sleeve bearing formed the revolute joint between the tool holder and slider, with its rotational axis aligned parallel to the spindle axis.

2.3. Actuator and Joint-Plate Design

The actuator was a double-acting round-body pneumatic cylinder with a 11.1 mm bore, 203.2 mm stroke, 4.83 mm rod diameter, and nitrogen actuation. Pressure on the two sides of the cylinder was independently controlled using manual regulators and digital pressure gauges. The chamber pressures were adjusted to account for the difference in effective volumes on the rod and non-rod sides. The pneumatic cylinder provided the adjustable resistance used to implement the human-derived target stiffness. As the piston moved during tool rotation, gas was compressed in one chamber while expanding in the other, producing a pressure difference and a restoring force that opposed the motion. The inherent mechanical resistance of the simulator was measured with the air supply disconnected so that no pneumatic pressure was applied to the cylinder. Trials were then conducted using the same tool displacement measurement used in the simulator experiments, and the baseline mechanical response was used to calculate an inherent stiffness of 519.6 N/m. This value includes resistance associated with the cylinder, slider, and hinge/bearing components,

including friction and stiction. The repeatability or uncertainty of this baseline stiffness measurement was not separately recorded.

Since the simulator itself had an inherent stiffness of 519.6 N/m, the cylinder pressure was selected to provide only the additional stiffness calculated for the desired operator stiffness. The required pressure for each experimental condition was calculated in MATLAB (R2025a) and set independently on the two sides of the cylinder.

The stiffness values used in this study are effective linear stiffnesses and are reported in N/m. For a target human stiffness K_S, the required pneumatic stiffness K was calculated by subtracting the inherent simulator stiffness:

$$K = K_S - K_{inherent} \quad (3)$$

Assuming isothermal gas compression, negligible leakage, the piston initially near half-stroke, and chamber volume much larger than the displaced volume, the pneumatic stiffness of the double-acting cylinder was approximated as:

$$K = 2A^2P_{in}/V_{in} \quad (4)$$

where A is the effective piston area, P_{in} is the initial cylinder pressure, and V_{in} is the initial chamber volume. The required pressure was therefore:

$$P_{in} = [(K_S - K_{inherent})V_{in}]/(2A^2) \quad (5)$$

The required pressure was calculated in MATLAB for each condition. The two chamber pressures were set independently to account for the difference between the rod and non-rod sides. The total stiffness achieved after pressure setting was not independently remeasured for each condition.

The threaded steel joint plate contained M6 × 1 mm holes and a 90° countersink on one face. During a normal fastening operation, the tool or workpiece must translate along the spindle axis as the fastener advances during rundown. Rather than translating the entire tool assembly, the joint plate was mounted on a linear slider and spring-loaded toward the tool. The compression spring was selected to maintain engagement between the driver bit and fastener while permitting the required axial motion throughout rundown and torque build-up. The spring-loaded joint-plate assembly is shown in Figure 3.

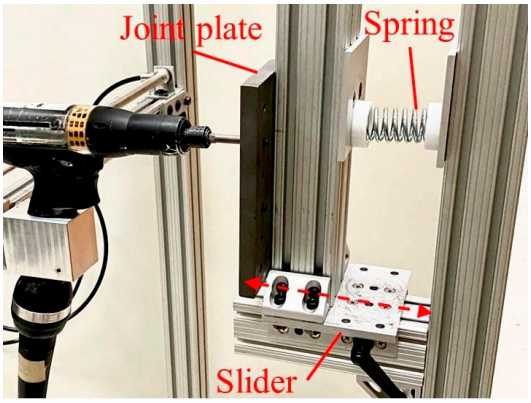


Figure 3. Spring-loaded joint-plate assembly. The joint plate translates toward the tool during fastener rundown to maintain engagement between the driver bit and fastener while the tool remains free to rotate about the spindle axis.

2.4. Human-Derived Stiffness Inputs

The operator mechanical properties used to evaluate the simulator were derived from the in vivo investigation reported previously [12]. In that study, experienced assembly-line

operators performed tightening tasks using the same pistol-grip tool at target torques of 5, 7.5, and 10 N·m and at four work locations corresponding to distinct wrist orientations. Tool torque and angular displacement were incorporated into a single-degree-of-freedom dynamic model to estimate upper-extremity stiffness and damping.

For the physical simulator described here, the relevant input was effective stiffness. Each participant and experimental condition generated a stiffness value that represented the resistance of the operator to tool-handle rotation [12]. These values were converted to an equivalent pneumatic resistance, allowing the simulator to represent experimentally observed human boundary conditions rather than an arbitrary spring constant. Although damping was quantified in the subsequent published human analysis [12], the simulator did not independently impose subject-specific damping; inherent friction and pneumatic effects provided some passive damping. The simulator is therefore described here as human-stiffness-based rather than as a complete stiffness-and-damping surrogate.

The same original in vivo trials supplied both the stiffness values used to parameterize the simulator and the corresponding human peak-displacement values used for comparison. The simulator trials themselves were separate bench tests. Thus, the human dataset used for the simulator–human comparison was not an independent external validation set; the agreement analysis applies to the same participant and location conditions used for simulator parameterization.

2.5. Instrumentation and Simulator Evaluation Procedure

Testing was performed using an Atlas Copco ETP ST32-10-I06 (Nacka, Sweden) DC-powered pistol-grip fastening tool, the same used in Arjun and Chandrashekar [12]. The tool was operated using an Atlas Copco Power Focus controller programmed using ToolsTalk PF (Version 2.21) software. Torque about the spindle axis was measured using the tool's integrated torque sensor, and spindle angular displacement was measured using the integrated rotary displacement transducer. The controller recorded the tightening data at 1000 Hz. For the simulator–human comparison, the fasteners used were M6 × 1 mm–16 mm long, flat-head, Torx plus drive, alloy steel screws, and a T30 Torx Plus Steel drive bit was used to fasten the screws (as in Arjun and Chandrashekar [12]).

The ETP ST32-10-I06 has a manufacturer-specified torque range of 3–11 N·m and a maximum speed of 1210 rpm [13]. Atlas Copco's angle accuracy guidance for tools equipped with an angle encoder specifies a maximum allowable angular deviation of ±5° over a 3600° rotation [14]. The native encoder resolution, controller–internal angle–filtering details, and trigger-delay setting were not available in the tool documentation. No additional filtering was applied after export for the peak-angle analysis reported here.

The evaluation procedure included simulator trials parameterized with the stiffness measured for each of the 10 operators at the corresponding torque and fastener location. At 7.5 N·m, stiffness values of all four operating locations (Low, High, Under, and Right) were available for every operator, giving 40 matched participant–location records. At 5 N·m, 30 matched location records were available across the same 10 operators; each operator was represented by two to four locations. Some of the 5 Nm operator trials could not be replicated on the simulator because the operator stiffness values were lower than the inherent stiffness of the system, resulting in negative pressure values required for simulation. For the primary simulator–human comparison, the available location-level values were averaged within each operator so that the paired statistical sample was n = 10 at each torque.

Once the stiffness values were set for each trial using pneumatic cylinders, the tool was triggered remotely using digital inputs to the Power Focus controller. Torque and angle were recorded throughout each fastening event at 1000 Hz. The peak handle displacement was calculated directly from the exported raw angle–time series as the maximum recorded

angle in each trial. The measured peak handle rotation was compared with the handle displacement of the corresponding in vivo trial [12]. The same peak definition—the maximum recorded angle in the exported angle–time series—was applied to the corresponding in vivo data. A paired t-test was used for statistical analysis, with the alpha value set at 0.05. In addition, agreement was summarized using 95% confidence intervals for the mean paired bias and Bland–Altman 95% limits of agreement, calculated as the mean bias ± 1.96 SD of the paired differences. The 5 and 7.5 N·m conditions were included because both were available in the original in vivo study and could be reproduced within the reliable mechanical operating range of the simulator prototype. The 10 N·m condition was not evaluated against the human measurements because the loading exceeded the reliable mechanical operating range of the simulator prototype. Sleeve-bearing failure and elevated slider friction occurred at the higher load and prevented valid reproduction of the 10 N·m human condition.

2.6. Parametric Testing of Fastening Variables

Following the simulator–human evaluation, the simulator was used for controlled tests at a target torque of 7.5 N·m. The stiffness was set 879 N/m, corresponding to the mean effective stiffness determined for the 7.5 N·m condition in the in vivo study [12], so that changes in handle motion reflected the engineering variable being tested rather than a change in simulated operator resistance. Four trials were included for each fastener and spindle-speed condition. Peak handle displacement from the raw angle–time series was the primary dependent variable. The fastener configurations used in these comparisons are shown in Figure 4.

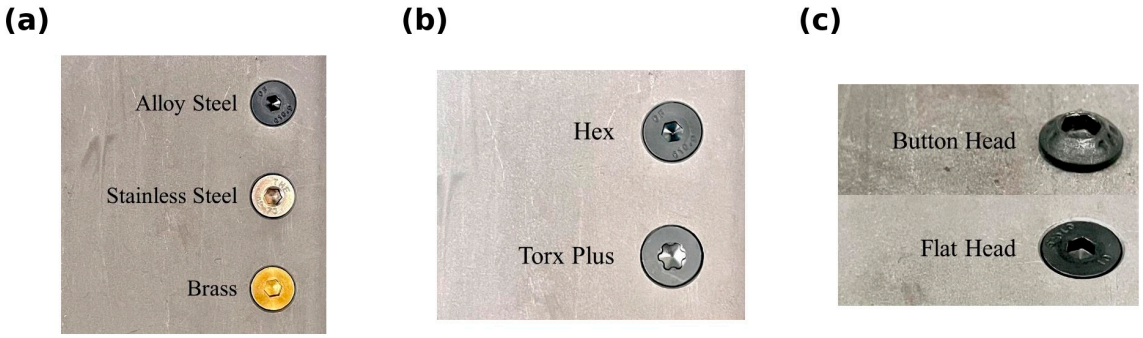


Figure 4. Fastener configurations evaluated using the simulator: (**a**) alloy steel, 18-8 stainless steel, and brass; (**b**) Hex and Torx Plus drive styles; and (**c**) button-head and flat-head geometries.

The parametric trials were conducted sequentially in condition blocks and were not randomized. Each test group (material, drive style, head type, and spindle speed) was evaluated separately, and the conditions within a group were completed in a fixed sequence. No separate remeasurement of the assembled system's stiffness was performed between these conditions; the same inherent stiffness correction was used when setting the cylinder pressure.

To test the effect of the fastener material on handle rotation, M6 × 1 mm flat-head fasteners manufactured from black-oxide alloy steel, 18-8 stainless steel, and brass were used. Their nominal elastic moduli were 200, 193, and 97 GPa, respectively. Equivalent Torx Plus fasteners were not commercially available across all three materials, so Hex-drive fasteners were used for the material comparison. The three fastener materials are shown in Figure 4a.

Two drive styles were compared: Torx Plus T30 and 4 mm Hex. The fasteners were black-oxide alloy steel and the remaining fastener characteristics were held as similar as

commercially available. Both driver bits were intended for powered fastening. The two drive geometries are shown in Figure 4b.

Flat-head and button-head fasteners were compared using black-oxide alloy steel and a 4 mm Hex drive. The flat-head fastener incorporated a 90° countersink, whereas the button-head fastener had a nominal head height of 3.3 mm. The principal mechanical distinction was the fastener-head/joint-plate contact geometry: the flat head engaged the countersunk joint plate through an inclined conical interface, whereas the button head produced a planar annular contact. The two head geometries are shown in Figure 4c.

The effect of spindle speed was evaluated at nominal settings of 100, 120, 140, and 160 rpm, while target torque was held at 7.5 N·m. Four trials were analyzed at each speed. Peak handle displacement was extracted directly from the raw angle–time series. An overall one-way ANOVA was used to test the speed effect; pairwise comparisons were treated as follow-up analyses. Tukey HSD tests were used for post hoc pairwise comparisons when the ANOVA was significant. Drive style and head type were compared with two-sided Welch two-sample t-tests. Statistical significance was set at $p < 0.05$.

3. Results

3.1. Simulator Evaluation Against Human Measurements

At 5 N·m, all 10 operators were represented by 30 matched participant–location records. After averaging the available matched locations within each operator, mean in vivo peak displacement was 44.85 ± 7.23°, compared with 59.57 ± 8.85° for the simulator. The mean positive bias was 14.72 ± 3.08° and the paired difference was significant ($p < 0.001$). At 7.5 N·m, all four locations were available for all 10 operators (40 matched participant–location records). Mean in vivo peak displacement across the participant means was 58.94 ± 7.47°, compared with 69.23 ± 4.76° for the simulator. The mean positive bias was 10.29 ± 9.52° and the paired difference was significant ($p = 0.0076$). These results are tabulated in Table 1.

Table 1. Comparison of peak handle displacement measured during human testing and simulator testing at target torques of 5 and 7.5 N·m. Values represent the mean ± SD. Bias represents the mean simulator–human difference; *p*-values are from paired t-tests.

Target Torque	Participants	Matched Location Records	Human Peak (°)	Simulator Peak (°)	Bias (°); Paired *p*
5 N·m	10	30	44.85 ± 7.23	59.57 ± 8.85	14.72; $p < 0.001$
7.5 N·m	10	40	58.94 ± 7.47	69.23 ± 4.76	10.29; $p = 0.0076$

Bland–Altman analysis of the participant-level paired differences gave a mean bias of 14.72° (95% CI: 12.52° to 16.92°) with 95% limits of agreement from 8.68° to 20.76° at 5 N·m. At 7.5 N·m, the mean bias was 10.29° (95% CI: 3.48° to 17.10°), with wider 95% limits of agreement from −8.37° to 28.95°.

Taken together, the updated n = 10 evaluation shows that the simulator does not provide unbiased absolute predictions of human peak displacement. Its more defensible use is as a repeatable comparative platform in which engineering conditions are tested against the same mechanical boundary condition.

3.2. Effect of Target Torque on Peak Handle Rotation

To find the effect of torque on peak handle rotation, the 7.5 N·m simulator mean for each operator was recalculated using the same locations available for that operator at 5 N·m. Mean peak displacement increased from 59.57 ± 8.85° at 5 N·m to 68.50 ± 4.43° at 7.5 N·m, an average increase of 8.93° (15.0%). The within-operator increase was significant ($p = 0.022$).

3.3. Effect of Fastener Material

Fastener material affected peak handle displacement at 7.5 N·m (one-way ANOVA, $p = 0.0047$). Mean peak displacement is shown in Table 2. Tukey HSD showed that peak handle rotation for alloy steel was lower than for stainless steel ($p = 0.004$) and brass ($p = 0.044$), while stainless steel and brass were not different ($p = 0.294$). The ordering did not follow the elastic modulus monotonically.

Table 2. Effect of fastener material on peak handle rotation during simulator testing. Elastic and shear moduli of the three fastener materials are shown for comparison. Peak rotation values are reported as mean ± SD from four trials (n = 4).

Fastener Material	Elastic Modulus (GPa)	Shear Modulus (GPa)	Peak Rotation (°), n = 4
Alloy steel	200	80	78.70 ± 0.99
18-8 stainless steel	193	77	85.68 ± 2.24
Brass	97	41	83.18 ± 2.93

3.4. Effect of Drive Style and Head Type

Torx Plus produced a mean peak handle displacement of 69.19 ± 2.52°, compared with 78.17 ± 3.01° for Hex drive (n = 4 trials per drive style). This corresponds to an 11.5% reduction with Torx Plus. The difference was significant ($p = 0.0041$).

Peak handle displacement was similar for the two head geometries. Flat-head fasteners produced 77.46 ± 3.49°, compared with 76.84 ± 1.70° for button-head fasteners (n = 4 trials per type). The difference was not significant ($p = 0.766$). These results are summarized in Figure 5.

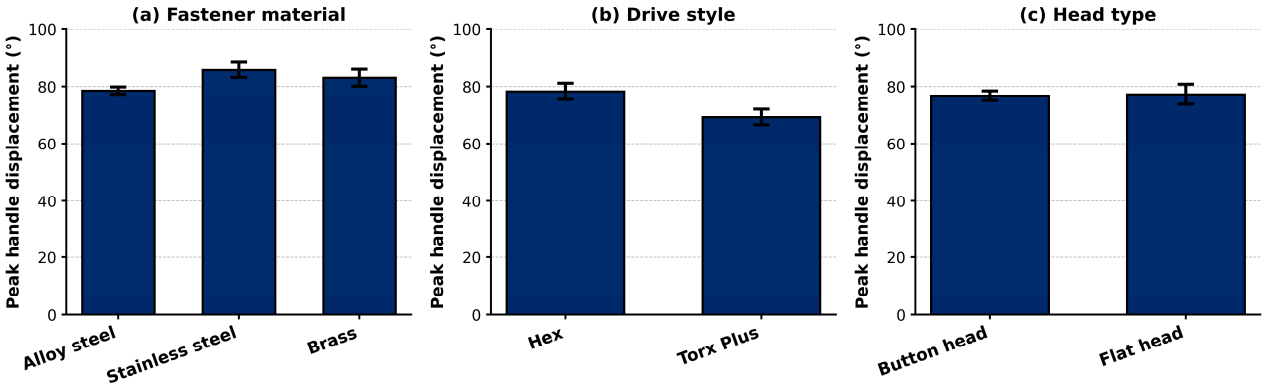


Figure 5. Summary of peak handle angular displacement for (**a**) fastener material, (**b**) drive style, and (**c**) head type. Trial-level points are plotted where available, with mean ± SD superimposed.

3.5. Effect of Spindle Speed

Spindle speed affected peak handle displacement ($p < 0.001$). Mean peak values were 74.81 ± 2.10° at 100 rpm, 78.92 ± 2.56° at 120 rpm, 78.23 ± 2.28° at 140 rpm, and 63.13 ± 1.15° at 160 rpm (n = 4 trials per speed). Tukey HSD showed no significant differences between 100, 120, and 140 rpm, whereas 160 rpm was lower than each of those conditions ($p < 0.001$). Torque build-up duration decreased progressively with speed: 227.3 ± 5.6 ms at 100 rpm, 191.8 ± 4.3 ms at 120 rpm, 164.0 ± 4.3 ms at 140 rpm, and 116.8 ± 1.3 ms at 160 rpm (ANOVA $p < 0.001$) (Figure 6).

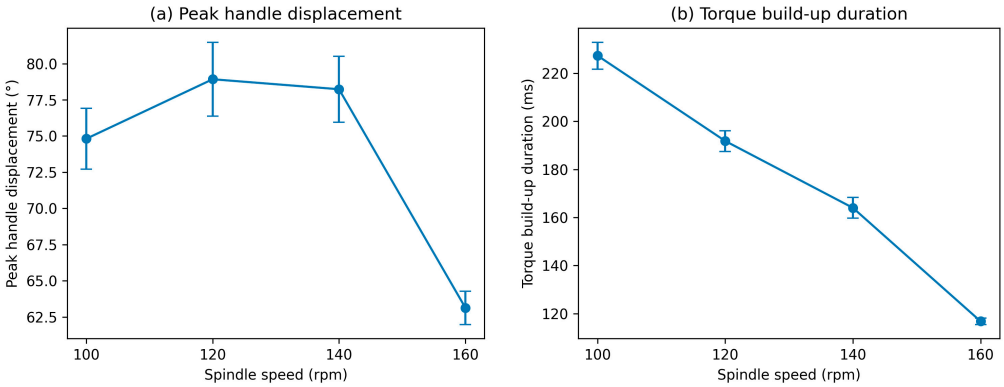


Figure 6. Peak handle displacement and torque build-up duration versus spindle speed (100, 120, 140, and 160 rpm), showing individual trials and mean ± SD.

Across the four repeated trials per parametric condition, the within-condition SD of peak rotation ranged from 0.99° to 3.49° for the fastener/drive/head comparisons and from 1.15° to 2.56° for the spindle-speed comparisons. These values describe trial-to-trial variability under the specific bench conditions tested.

A representative 7.5 N·m simulator tightening cycle is shown in Figure 7 to illustrate the torque-time and angular displacement–time response used to determine peak displacement.

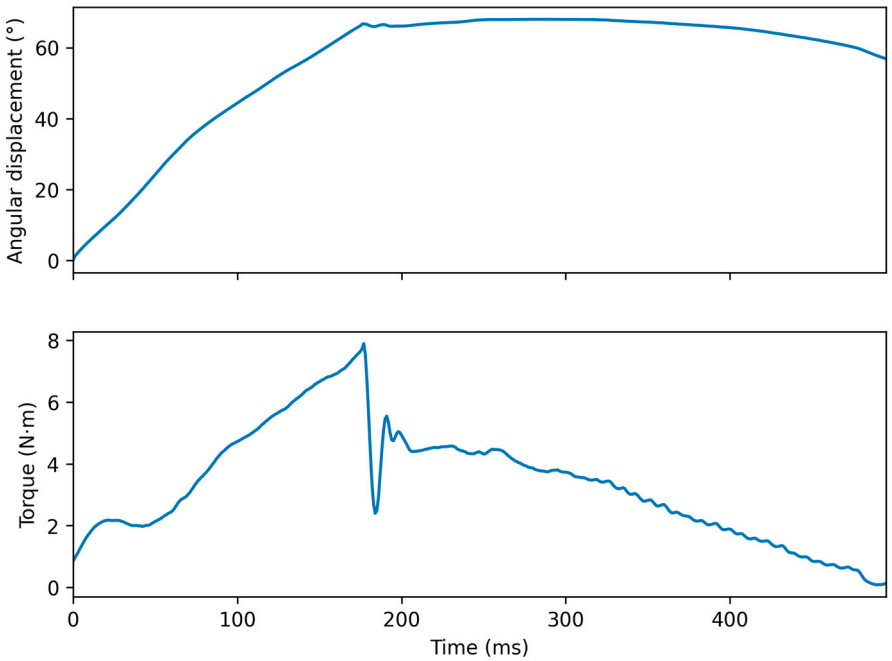


Figure 7. Representative torque–time and angular displacement–time histories for one simulator trial at a target torque of 7.5 N·m. Peak handle displacement was defined as the maximum recorded angular displacement in the exported angle–time series.

4. Discussion

4.1. Simulator Human Agreement and Sources of Bias

The comparison with human data shows that the present stiffness-only simulator should not be treated as an absolute surrogate for the operator. This is consistent with hand–arm models presented by Lin et al. [7–9], in which tool response depends on stiffness, damping, and effective inertia, and with the right-angle simulator of Ay et al. [10,11], which also treated the operator as a dynamic mechanical system. The positive displacement bias at both torque levels indicates that matching effective stiffness alone was not

sufficient to reproduce the complete transient human response. The more appropriate use of the current device is therefore controlled relative screening under a fixed mechanical boundary condition.

The distinguishing feature of the simulator is that its resistance was derived from measurements obtained during actual tool use. Human experiments remain essential for identifying physiologically representative stiffness and damping and for determining how these properties vary with torque, posture, and operator characteristics [12]. Once those properties are known, however, a physical surrogate allows engineering variables to be altered while the human mechanical boundary condition is held constant.

This distinction is important for the parametric experiments. A fixed bias in the simulator is much less problematic when two fasteners or tool settings are compared using the same actuator setting and the same mechanical rig. Under those conditions, the main question is the difference between engineering conditions, not whether the simulator reproduces the absolute human angle. This role in relative comparison is the strongest application of the current prototype. Using the simulator for early-stage screening also reduces the need for repeated human testing of tool and fastener combinations whose reaction characteristics have not yet been established.

The simulator–human comparison shows that there is a clear positive bias: on average, the rig rotated farther than the corresponding human-held tool. This suggests that a single stiffness-based mechanical representation does not capture all of the active and torque-dependent features of the human response. The simulator does, however, remove much of the uncontrolled variability associated with grip strategy, anticipation, fatigue, and voluntary muscle activation, which is useful when the aim is to compare engineering conditions rather than to predict an individual worker's response.

The total observed bias can be quantified, but the contribution of each mechanism cannot be separated from the present measurements. The mean simulator–human bias was +14.72° at 5 N·m and +10.29° at 7.5 N·m. Omitting subject-specific damping would tend to reduce transient resistance and could increase peak rotation, whereas friction and stiction add mechanical resistance and may partially oppose that effect. The achieved total stiffness after each pressure setting was not independently measured, so stiffness-setting errors could also have contributed. In addition, the single-degree-of-freedom representation excludes coupled and active motion of the wrist, elbow, shoulder, and torso described in human hand–arm models [7–10].

Because the stiffness inputs and reference human peak angles came from the same original participant–location trials, this comparison is an in-sample agreement evaluation rather than an independent external validation. The wider Bland–Altman limits of agreement at 7.5 N·m also show that the simulator–human deviation was not constant across participants. The present data therefore do not establish a stable bias that can be transferred to untested fastening configurations.

4.2. Effect of Target Torque

Peak simulator rotation increased from 59.57° at 5 N·m to 68.50° at 7.5 N·m when the 7.5 N·m values were calculated using the same locations available for each operator at 5 N·m. The mean increase was 8.93° (15.0%) and was significant in the paired participant-level comparison ($p = 0.022$). This direction is consistent with the greater reaction moment expected at the higher target torque. Because the 5 N·m dataset did not contain all four locations for every operator, the magnitude of the increase should still be interpreted within the available matched-location set.

The increase with torque is consistent with previous torque tool studies showing that handle response depends on the magnitude and time course of torque build-up [2,5,6].

Lin et al. [5,6] also showed that joint hardness and working posture affect handle displacement and operator response, confirming that target torque alone does not determine the mechanical exposure.

Target torque is normally dictated by assembly requirements and cannot simply be reduced for ergonomic reasons. The more useful implication is that higher-torque tasks provide less margin for other design features that amplify reaction. Conversely, when multiple fastening solutions satisfy the same structural requirement, reducing joint compliance or improving torque-transfer characteristics may provide an ergonomic benefit without changing the final torque requirement.

4.3. Effect of Fastener Material

The updated material results do not support a simple modulus-based explanation. Alloy steel produced the lowest peak rotation, but stainless steel produced the highest response, even though its nominal elastic modulus is close to that of alloy steel. Brass, despite having a much lower modulus, fell between the two. Surface condition is one possible contributor: the stainless-steel fasteners were passivated, whereas the alloy-steel fasteners had a black-oxide finish. Friction, seating behavior, thread condition, and manufacturing tolerances could therefore contribute to the observed torque–angle response. Those quantities were not measured directly, so this explanation remains a hypothesis rather than a demonstrated mechanism.

Previous work has emphasized the effects of joint hardness and torque-build-up behavior rather than fastener material in isolation [5,6]. The present non-monotonic material result is consistent with treating the fastener and joint as part of the complete dynamic fastening system rather than using elastic modulus alone as a predictor of handle response.

For a fastener subjected to torsion, angular twist can be approximated using $\varphi = TL/(JG)$, where T is the applied torque, L is the fastener length, J is the polar second moment of area, and G is the shear modulus. This relationship explains why fastener compliance was considered as a possible contributor to tool reaction. However, the updated experimental ordering did not follow G monotonically: stainless steel and alloy steel have similar nominal shear moduli, yet their measured peak rotations differed, while brass fell between them. The torsion–stiffness relationship is therefore useful in terms of background mechanics, but it does not by itself explain the present material result.

The result should not be interpreted as a recommendation to choose fastener materials primarily on ergonomic grounds. Strength, preload retention, fatigue, corrosion, cost, manufacturability, and service environment remain dominant design constraints. Instead, the findings show that material selection can have a secondary ergonomic consequence and should be recognized as part of the complete tool–fastener–joint system.

4.4. Effect of Drive Style and Head Type

Drive style produced the clearest fastener-level effect. Torx Plus reduced peak handle rotation by 11.5% relative to Hex under the same 7.5 N·m condition. Differences in contact geometry between the driver and recess provide a plausible mechanical explanation because they can alter local deformation, slip, and torque transfer. The present study measured the overall system response rather than contact stress at the bit-fastener interface, so the specific mechanism should be tested directly before it is treated as established.

Most previous torque tool studies have focused on operator posture, joint hardness, or overall tool dynamics [2,5,6]. The drive interface comparison here extends that work to a fastener-level design variable, while the mechanism responsible for the measured difference remains to be established.

From a practical standpoint, the measured difference indicates that drive style is not mechanically neutral with respect to the tool handle reaction. Drive selection is normally based on torque capacity, accessibility, wear, manufacturability, and resistance to stripping; the present results suggest that reaction behavior may also be worth considering when otherwise acceptable alternatives are available.

The updated head-type experiment did not show a measurable difference between the flat-head and button-head fasteners. This result does not support the earlier contact-area hypothesis under the present 7.5 N·m test condition. It also should not be interpreted as evidence that head geometry can never affect tool reaction. The effect may depend on joint material, seating geometry, friction, torque level, or other fastener characteristics that were not varied here.

The nominal contact geometries were quite different, but the measured peak rotations were nearly the same. A larger set of head geometries, torque levels, and joint materials would be needed to determine whether head-contact area has a smaller effect that was not resolved in this experiment.

4.5. Effect of Spindle Speed

Spindle speed produced the largest change in the parametric dataset, but the response was not monotonic. Peak rotation was similar from 100 to 140 rpm and then dropped sharply at 160 rpm. Torque build-up duration, in contrast, decreased steadily as speed increased, from about 227 ms at 100 rpm to 117 ms at 160 rpm. The abrupt change in angle at 160 rpm is therefore not explained simply by a proportional shortening of the build-up interval. Before this is interpreted as an ergonomic benefit of higher speed, the 160rpm torque angle traces and the mechanical motion of the simulator should be checked for controller behavior, actuator lag, or other dynamic limits.

This result should be viewed in the context of earlier research showing that torque build-up characteristics influence handle response [2,5]. In the present dataset, build-up duration shortened progressively with speed, but peak angle did not change monotonically, so spindle speed alone should not be treated as the cause of the lower value at 160 rpm.

4.6. Practical and Design Implications

A central practical implication is that the same final tightening torque does not necessarily imply equal reaction (kickback) exposure to the operator. The fastening operation is a dynamic system in which the motor, controller, spindle, driver, fastener, joint, and human boundary condition interact. Changes in fastener or joint design can therefore alter the transient pathway by which torque is transmitted and resisted.

This suggests a design-for-ergonomics framework in which fastener and joint characteristics are considered alongside tool and workstation variables. In an assembly-line environment, even modest reductions in reaction per fastening cycle may become meaningful when a worker performs hundreds of repetitions per shift.

Peak handle rotation is one kinematic descriptor of torque tool reaction. Previous studies have considered handle displacement together with reaction force, muscle activity, and discomfort [2,3,5], so peak rotation should be interpreted as one component of biomechanical exposure rather than as a direct measure of musculoskeletal injury risk.

From a practical perspective, the simulator could be used as a screening tool during the design and planning of industrial fastening operations. Engineers could systematically compare candidate fasteners, drive styles, joint configurations, spindle speeds, and tightening strategies under the same human-derived mechanical boundary condition before these configurations are implemented on an assembly line. Configurations that produce lower peak handle rotation may be considered potentially more favorable from an ergonomic

standpoint because they reduce the magnitude of tool motion that must be resisted by the operator. However, peak handle rotation is only one measure of biomechanical exposure, and the simulator is not intended to directly predict musculoskeletal injury risk. Rather, it can help to identify promising fastening configurations for subsequent ergonomic assessment and, where appropriate, validation with human operators.

4.7. Limitations

The current simulator has several limitations. First, it represents the operator using a single degree of freedom. Actual tool use involves coupled motion of the wrist, elbow, shoulder, and torso and can include rotations and translations outside the spindle axis. The current device is therefore a surrogate for the dominant handle rotation rather than a complete musculoskeletal representation.

Second, human mechanical behavior is active, nonlinear, and time dependent. The simulator applied an approximately linear stiffness and did not independently reproduce the subject-specific damping quantified in the later in vivo publication. Future versions should incorporate a controllable damping element, potentially using a servo-controlled actuator or variable damper, and they should examine nonlinear stiffness over the complete torque-build-up interval.

Because subject-specific damping was not imposed and the achieved total stiffness after each pressure setting was not independently verified, the separate quantitative contributions of damping error and stiffness-setting error to the observed displacement bias cannot be determined from the present data.

Third, friction and stiction were present in the pneumatic cylinder and slider. Their contribution was partly addressed by measuring the inherent simulator stiffness (519.6 N/m), but they may have contributed to the remaining individual-level disagreement. Improving bearings, guide elements, and actuator technology should reduce this effect.

Fourth, the prototype could not reliably reproduce the 10 N·m condition because of sleeve-bearing failure and excessive friction under higher load. The conclusions should therefore be restricted to the tested 5–7.5 N·m range until the structure and bearings are upgraded and a higher-torque evaluation is completed. The evaluated operating range of the current prototype is therefore 5–7.5 N·m, and extrapolation beyond this range is not supported by the present study.

Fifth, only three fastener materials, two drive styles, and two head geometries were available for comparison, and commercial availability prevented every design feature from being held identical. Each parametric condition was repeated four times, which is adequate for identifying large differences but provides limited precision for smaller effects. At 5 N·m, 10 participant–location simulator records were unavailable. All 10 participants were still represented, and the paired simulator–human comparison was therefore performed on participant-level means calculated from the available matched locations. The parametric trials were conducted in fixed sequential blocks rather than randomized order; therefore, progressive effects such as temperature, friction, wear, or pneumatic behavior cannot be ruled out as contributors to condition differences.

Human reference measurements were not available for every parametric fastening condition, so the stability of the simulator–human bias across those conditions could not be established. The comparative findings should therefore be interpreted only as relative bench-test differences under the fixed mechanical boundary conditions used here.

Finally, peak angular displacement was the primary output. Angular velocity, acceleration, reaction impulse, torque build-up time, clamp force, and energy transfer may provide additional insight into the potential ergonomic significance of the reaction. Incorporating these measures would strengthen the link between bench-test response and

operator exposure. A next-generation validation should incorporate controlled damping, lower-friction bearings or actuation, direct verification of achieved stiffness, higher-torque capability, additional fastener and joint configurations, and comparison of angular velocity, acceleration, reaction impulse, and energy transfer against an independent human dataset.

5. Conclusions

A human-stiffness-based physical simulator was developed for DC-powered pistol-grip fastening. Evaluation against human measurements from all 10 operators showed that the simulator systematically overpredicted peak human handle displacement, with mean participant-level biases of 14.72° at 5 N·m and 10.29° at 7.5 N·m. The current prototype should therefore be used primarily for controlled relative comparisons between fastening parameters rather than direct predictions of absolute human response. The current prototype was evaluated only over 5–7.5 N·m, and extrapolation beyond this range is not supported.

Under a fixed 7.5 N·m condition, Torx Plus produced 11.5% less peak rotation than Hex drive. Fastener material also affected rotation, although the non-monotonic pattern shows that elastic modulus alone is not a sufficient explanation. Flat-head and button-head fasteners produced similar peak rotations. Rotation fell sharply at 160 rpm, but this isolated high-speed finding should be verified before it is used as a design recommendation. These parameter findings are limited to the specific tool, fastener, joint, and operating conditions tested.

The main value of the simulator is that it holds the mechanical representation of the operator constant while fastener or tool parameters are changed. This makes it useful for screening fastening system design choices and identifying conditions that warrant later testing with human subjects. Accordingly, the device should be considered a human-stiffness-based screening platform for relative comparisons under fixed boundary conditions, not an absolute predictor of human displacement or musculoskeletal injury risk.

Author Contributions: Conceptualization, R.A. and N.C.; methodology, R.A. and N.C.; software, R.A.; validation, P.B., R.A. and N.C.; formal analysis, R.A. and N.C.; investigation, P.B. and R.A.; resources, N.C.; data curation, P.B.; writing—original draft preparation, N.C.; writing—review and editing, R.A. and N.C.; visualization, N.C. and R.A.; supervision, N.C.; project administration, N.C.; funding acquisition, N.C. All authors have read and agreed to the published version of the manuscript.

Funding: This research was funded by the Natural Sciences and Engineering Research Council of Canada and Honda Canada Manufacturing, Alliston, ON (CRDPJ 535905-18).

Institutional Review Board Statement: The study was conducted in accordance with the Declaration of Helsinki. The original in vivo data used to derive operator stiffness were collected under a protocol approved by the Research Ethics Board of the University of Waterloo (31571, 17 January 2018); no new human-subject testing was performed for this study.

Informed Consent Statement: Not applicable—no new human participants were involved in this study. Informed consent for the original in vivo data collection was obtained as reported in [12].

Data Availability Statement: The data supporting the findings of this study are available from the corresponding author upon reasonable request.

Acknowledgments: The authors acknowledge Honda of Canada Manufacturing (HCM), Alliston, Ontario, and the participating workers for supporting the original in vivo study.

Conflicts of Interest: The authors declare no conflicts of interest. The sponsors had no role in the design, execution, interpretation, or writing of the study.

References

1. Potvin, J.R.; Agnew, M.J.; Ver Woert, C. An ergonomic comparison of pneumatic and electrical pistol grip hand tools. *Int. J. Ind. Ergon.* **2004**, *34*, 467–478. [CrossRef]
2. Kihlberg, S.; Kjellberg, A.; Lindbeck, L. Pneumatic tool torque reaction: Reaction forces, displacement, muscle activity and discomfort in the hand-arm system. *Appl. Ergon.* **1993**, *24*, 165–173. [CrossRef] [PubMed]
3. Armstrong, T.; Bir, C.; Foulke, J.; Martin, B.; Finsen, L.; Sjogaard, G. Muscle responses to simulated torque reactions of hand-held power tools. *Ergonomics* **1999**, *42*, 146–159. [CrossRef] [PubMed]
4. Ku, C.H.; Radwin, R.G.; Karsh, B.T. Power hand tool kinetics associated with upper limb injuries in an automobile assembly plant. *J. Occup. Environ. Hyg.* **2007**, *4*, 391–399. [CrossRef] [PubMed]
5. Lin, J.H.; McGorry, R.W.; Chang, C.C.; Dempsey, P.G. Handle displacement and operator responses to pneumatic nutrunner torque buildup. *Appl. Ergon.* **2006**, *37*, 367–376. [CrossRef] [PubMed]
6. Lin, J.H.; McGorry, R.W.; Chang, C.C.; Dempsey, P.G. Effects of user experience, working posture and joint hardness on powered nutrunner torque reactions. *Ergonomics* **2007**, *50*, 859–876. [CrossRef] [PubMed]
7. Lin, J.H.; Radwin, R.G.; Richard, T.G. Dynamic biomechanical model of the hand and arm in pistol grip power handtool usage. *Ergonomics* **2001**, *44*, 295–312. [CrossRef] [PubMed]
8. Lin, J.H.; Radwin, R.G.; Richard, T.G. A single-degree-of-freedom dynamic model predicts the range of human responses to impulsive forces produced by power hand tools. *J. Biomech.* **2003**, *36*, 1845–1852. [CrossRef] [PubMed]
9. Lin, J.H.; Radwin, R.G.; Richard, T.G. Handle dynamics predictions for selected power hand tool applications. *Hum. Factors* **2003**, *45*, 645–656. [CrossRef] [PubMed]
10. Ay, H.; Sommerich, C.M.; Luscher, A. Linear modeling of human hand-arm dynamics relevant to right-angle torque tool interaction. *Hum. Factors* **2013**, *55*, 893–910. [CrossRef] [PubMed]
11. Ay, H.; Luscher, A.; Sommerich, C.M. A dynamic simulator for the ergonomics evaluation of powered torque tools for human assembly. *Assem. Autom.* **2017**, *37*, 1–12. [CrossRef]
12. Arjun, R.; Chandrashekar, N. Effects of DC-powered pistol grip tool location and orientation on operator upper extremity stiffness and damping. *Appl. Ergon.* **2025**, *126*, 104491. [CrossRef] [PubMed]
13. Atlas Copco. ETP ST32-10-I06, Product No. 8433 2214 63 Technical Specifications. Available online: https://www.atlascopco.com/en-us/itba/products/assembly-solutions/electric-assembly-tools/etp-st32-10-i06-sku8433221463 (accessed on 13 October 2026).
14. Atlas Copco. Accuracy Guide. Atlas Copco Industrial Technique AB. Available online: https://www.atlascopco.com/content/dam/atlas-copco/local-countries/united-states/documents/itba/Atlas%20Copco%20Accuracy%20Guide.pdf (accessed on 13 October 2026).

Disclaimer/Publisher's Note: The statements, opinions and data contained in all publications are solely those of the individual author(s) and contributor(s) and not of MDPI and/or the editor(s). MDPI and/or the editor(s) disclaim responsibility for any injury to people or property resulting from any ideas, methods, instructions or products referred to in the content.